LASER INTERFEROMETER GRAVITATIONAL WAVE OBSERVATORY
- LIGO -
CALIFORNIA INSTITUTE OF TECHNOLOGY
MASSACHUSETTS INSTITUTE OF TECHNOLOGY

Technical Note **LIGO-T1300155–v1** 2013/05/11

Alignment sensing control signals of DRMI

K Kokeyama, A Effler, and L Barsotti

Distribution of this document:

LIGO Science Collaboration

California Institute of Technology
LIGO Project, MS 100-36
Pasadena, CA 91125
Phone (626) 395-2129
Fax (626) 304-9834
E-mail: info@ligo.caltech.edu

Massachusetts Institute of Technology
LIGO Project, NW22-295
Cambridge, MA 02139
Phone (617) 253-4824
Fax (617) 253-7014
E-mail: info@ligo.mit.edu

LIGO Hanford Observatory
PO Box 159
Richland, WA 99352
Phone (509) 372-8106
Fax (509) 372-8137
E-mail: info@ligo.caltech.edu

LIGO Livingston Observatory
19100 LIGO Lane
Livingston, LA 70754
Phone (225) 686-3100
Fax (225) 686-7189
E-mail: info@ligo.caltech.edu

http://www.ligo.caltech.edu/

Contents

1 Introduction

This document shows the alignment signal matrix for dual-recycling Michelson Interferometer (DRMI) for Advanced LIGO (aLIGO) Livingston corner Michelson commissioning. The calculations are done by the simulation software Finesse. All the scripts can be found MIT CVS `iscmodeling/Finesse/L1/ASC`.

There are several wave front sensors (WFS) available for the corner Michelson commissioning, as listed in Table. 1. There are four sets of WFS; in-vacuum or in-air AS path and in-vacuum or in-air REFL path, and there is a set of DC QPDs in POP path. The path including Gouy phase telescopes are shown in Fig. 1. Each path has WFSA and WFSB which are 90 ° separated in the accumulated Gouy phase. In the simulation, any fraction of the pick-off optics are taken out, except there is a 50 % pick-off beamsplitter to send the REFL beam to the in-vac or in-air REFL sensors. Table. 2 shows the DC power at each detection port, when the input beam power is 2 W.

The configuration of the corner Michelson interferometer in the simulation is DRMI with carrier fields locked both on PRC and SRC. Note that the DRMI model in the simulation has astigmatisms due to the foldings of PRC and SRC.

2 In-vacuum AS path

The Gouy phase telescope design and the beam parameters for in-vacuum (in-vac) AS path are shown in the left panel of Fig. 1 and in [1]. After transmitting SRM, the laser field passes through the tip-tilt M1 (Rc = 4.6 m) and M2 (Rc = 1.7 m), a flat steering beamsplitter M3, and a lens L101 (f = 0.334 m). In the simulation, the two tip-tilt mirrors (M1 and M2)

Path	Mode	Location
In-vacuum AS	Science mode	HAM6
In-vacuum REFL	Science mode	HAM1
In-air AS	Acquisition mode	ISCT6
In-air REFL	Acquisition mode	ISCT1
In-vacuum POP (DC QPD)	Science mode	HAM2

Table 1: WFS path list for the corner part of the interferometer. Some of them might not be used for the DRMI commissioning time. Each WFS path has WFSA and WFSB which are 90 $^\circ$ separated in the accumulated Gouy phase.

Path	Power
In-vacuum AS	3.1 μW
In-vacuum REFL	0.057 W
In-air AS	3.1 μW
In-air REFL	0.057 W
In-vacuum POP (DC QPD)	0.013 W

Table 2: DC power at each detection port, in the simulation. No fraction of the pick-off optics are considered, except there is a 50 % pick-off beamsplitter to send the REFL beam to the in-vac or in-air REFL sensors.

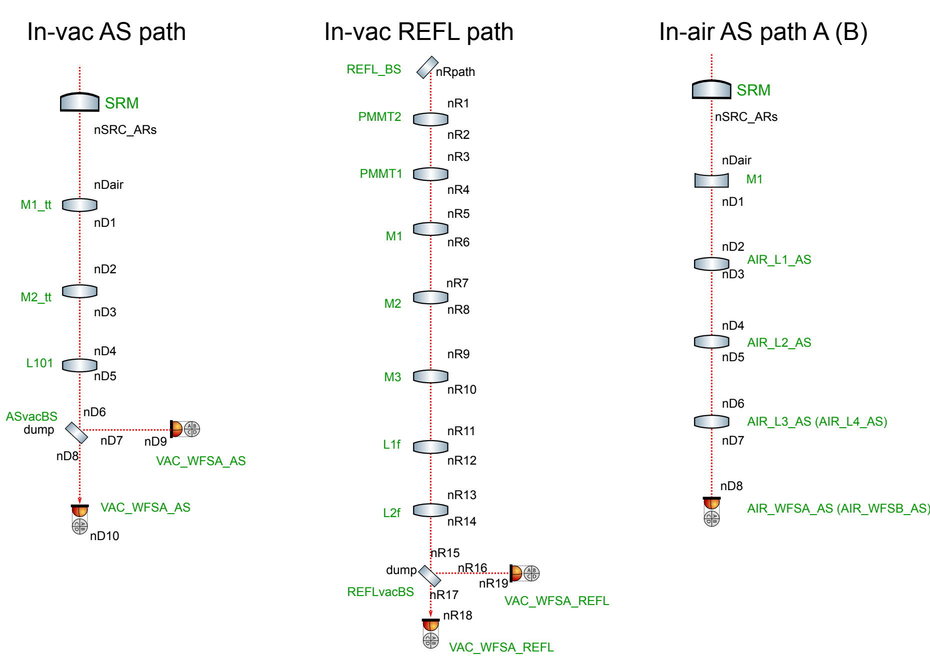

Figure 1: In-vacuum AS, In-vacuum REFL, In-air AS path. Node names used in the simulation are shown as well.

Label	z [m]	beam radius [mm] (x, y)	Gouy phase from SRM [deg] (x,y)
SRM	0	(2.00, 2.12)	(0, 0)
WFSA	6.46	(0.32, 0.31)	(242, 239)
WFSB	6.743	(0.301, 0.309)	(328, 331)

Table 3: Beam size and accumulated Gouy phases in in-vac AS path obtained by the simulation.

are approximated as lenses with the focal lengths of the half radius of curvature, and tip-tilt M3 is abbreviated so that we don't take into account any additional astigmatism due to the incident angle of the telescopes, and also the pick-off factors at the WFS path.

The obtained beam parameters are listed in Table. 3, showing a good agreement with the design values in [1].

The calculated ASC matrices in in-vac AS are shown from Table. 4 to Table. 7. They are shown in [W/rad], and any pick-offs at the detection port is taken out, i,e, WFS senses all the power at AS port. In this detection port, because f_1 sideband does not leak to the AS port, signals are obtained only by f_2 demodulation. The strongest ITM and BS signals at in-vac AS port are plotted in Fig. **??** as a function of the accumulated Gouy phase (i.e., the WFS position).

WFSA, Demod by 36 MHz [W/rad]		
	yaw	pitch
ITMy	-0.811	-0.839
ITMx	0.785	-0.818
BS	-0.760	1.13
PRM	-0.000935	0.000941
PR2	0.00307	-0.00303
PR3	0.0267	0.0263
SRM	-0.000759	0.000646
SR2	-0.00927	-0.00837
SR3	-0.0607	0.0548

Table 4: In-vacuum AS WFSA, demodulated by 36 MHz. Demodulation phases are optimzed so that each signal is maximum.

WFSA, Demod by 45 MHz [W/rad]		
	yaw	pitch
ITMx	2260	-2140
ITMy	-2260	-2140
BS	-2190	2980
PRM	-0.0301	0.0263
PR2	0.151	-0.132
PR3	1.31	1.14
SRM	0.000408	-0.000403
SR2	0.00307	0.00303
SR3	0.0205	-0.0201

Table 5: In-vacuum AS WFSA, demodulated by 45 MHz. Demodulation phases are optimzed so that each signal is maximum.

3 In-vacuum REFL path

The Gouy phase telescope design and the beam parameters for in-vacuum REFL path are shown in the middle panel of Fig. 1. There are seven telescopes, pre-mode-matching telescope 1 (PMMT1, Rc = -6.24 m), PMMT2 (Rc = 12.8 m), tip-tilt M1 (Rc = 1.7 m), M2 (Rc = -0.6 m), M3 (Rc = 1.7m), and two lenses, L1f (f = 0.333 m) and L2f (f = -0.167 m). Please

WFSB, Demod by 36 MHz [W/rad]		
	yaw	pitch
ITMy	0.578	0.626
ITMx	-0.600	0.645
BS	0.554	-0.860
PRM	0.000972	-0.000968
PR2	-0.00495	0.00489
PR3	-0.0430	-0.0426
SRM	0.000631	-0.000559
SR2	0.00418	0.00374
SR3	0.0275	-0.0245

Table 6: In-vacuum AS WFSB, demodulated by 36 MHz.

WFSB, Demod by 45 MHz [W/rad]		
	yaw	pitch
ITMx	2580	-2270
ITMy	-2580	-2260
BS	-2500	3160
PRM	-0.0366	0.0284
PR2	0.191	-0.148
PR3	1.66	1.29
SRM	0.00115	-0.000831
SR2	0.00864	0.00625
SR3	0.0560	-0.0405

Table 7: In-vacuum AS WFSB, demodulated by 45 MHz.

Label	z [m]	beam radius [mm] (x, y)	Gouy phase from PRM [deg] (x,y)
Telescope M1	0	(2.01, 2.04)	(26.1, 24.8)
WFSA	3.26	(0.330, 0.331)	(223, 221)
WFSB	3.63	(0.378, 0.378)	(314, 315)

Table 8: Beam parameters in in-vac REFL path obtained by the simulation.

see [2] for the spacial parameters. Similarly to the in-vac AS path case, all the telescopes are included as lenses in the simulation. The obtained beam size and the accumulated Gouy phase are listed in Table. 8.

The calculated ASC matrices in in-vac REFL are shown from Table. 9 to Table. 12. They are shown in [W/rad], and any pick-offs at the detection port is taken out, i,e, WFS senses all the power at REFL port. In this detection port, PR3 misalignment signals are the strongest of all the signals. The second strongest signals are the ITM and BS signals.

4 In-air REFL

There is the in-air REFL path on ISCT1. The detailed parameters are to be determined. The following matrices are example using Kiwamu's solution (C). The estimated q parameter at the edge of ISCT1 is $q = 1.13 + 13i$ ($z = 0$). There are two lenses, f0_airREFL (f = 0.6785 m at z = 0.677 m) and f1_airREFL (f = -0.5727 m at z = 1.0323 m). The beam waist after these lenses are about 250 μm. The ASC matrices at in-air REFL port are shown in Table. 13 to Table. 16

WFSA, Demod by 9 MHz [W/rad]		
	yaw	pitch
ITMx	11400	-11000
ITMy	11400	10900
BS	11300	-14500
PRM	-59.6	58.2
PR2	3950	-3810
PR3	26100	26400
SRM	-0.000764	0.000774
SR2	-0.00575	-0.00583
SR3	-0.0377	0.0382

Table 9: In-vacuum REFL WFSA, demodulated by 9 MHz.

WFSA, Demod by 45 MHz [W/rad]		
	yaw	pitch
ITMx	11500	-11000
ITMy	11400	11000
BS	11300	-14500
PRM	-59.6	58.2
PR2	3950	-3810
PR3	26100	26400
SRM	0.0638	-0.0557
SR2	0.480	0.419
SR3	3.03	-2.67

Table 10: In-vacuum REFL WFSA, demodulated by 45 MHz.

WFSB, Demod by 9 MHz [W/rad]		
	yaw	pitch
ITMx	13900	-12800
ITMy	13900	12800
BS	13400	-18200
PRM	-1280	1200
PR2	4210	-4030
PR3	41700	39400
SRM	-0.000803	0.000790
SR2	-0.00604	-0.00594
SR3	-0.0395	0.0388

Table 11: In-vacuum REFL WFSB, demodulated by 9 MHz.

WFSB, Demod by 45 MHz [W/rad]		
	yaw	pitch
ITMx	13900	-12800
ITMy	13900	12800
BS	13400	-18200
PRM	-1280	1200
PR2	4210	-4040
PR3	41700	39400
SRM	0.0463	-0.0402
SR2	0.348	0.303
SR3	2.30	-2.00

Table 12: In-vacuum REFL WFSB, demodulated by 45 MHz.

WFSA, Demod by 9 MHz [W/rad]		
	yaw	pitch
ITMx	-16700	15300
ITMy	-16700	-15300
BS	-16200	21300
PRM	540	-500
PR2	-5270	4970
PR3	-46000	-43500
SRM	0.000957	-0.000936
SR2	0.00720	0.00704
SR3	0.04702	-0.0460

Table 13: In-air REFL WFSA, demodulated by 9 MHz.

WFSA, Demod by 45 MHz [W/rad]		
	yaw	pitch
ITMx	-16700	15300
ITMy	-16700	-15300
BS	-16200	21300
PRM	540	-500
PR2	-5270	4970
PR3	-46100	-43500
SRM	-0.0767	0.0655
SR2	-0.577	-0.493
SR3	-3.77	3.22

Table 14: In-air REFL WFSA, demodulated by 45 MHz.

WFSA, Demod by 9 MHz [W/rad]		
	yaw	pitch
ITMx	-7830	7400
ITMy	-7820	-7410
BS	-7590	10300
PRM	1160	-1120
PR2	-2470	2410
PR3	-21600	-21100
SRM	0.000572	-0.000581
SR2	0.00430	0.00437
SR3	0.0281	-0.0286

Table 15: In-air REFL WFSB, demodulated by 9 MHz.

WFSA, Demod by 45 MHz [W/rad]		
	yaw	pitch
ITMx	-7840	7420
ITMy	-7820	-7410
BS	-7590	10300
PRM	1170	-1120
PR2	-2470	2410
PR3	-21600	-21100
SRM	-0.0200	0.0176
SR2	-0.150	-0.133
SR3	-0.983	0.867

Table 16: In-air REFL WFSB, demodulated by 45 MHz.

5 In-air AS

There will be in-air AS path on ISCT6. The two solutions of the beam parameters are summarized in [1]. Here, we used the first solution for the ASC matrix calculation, and its setup is shown in the right panel of Fig. 1. The beam transmits a curved mirror M1 (common as in-vacuum AS path), then two lenses AIR_L1_AS ($f = 1.146$m), AIR_L2_AS ($f = 0.556$m). Then there is a lens AIR_L3_AS ($f = -0.0556$m) before in-air AS WFSA, and AIR_L4_AS ($f = -0.111$m) before in-air WFSB.

Table. 17 and Table. 20 are the sensing matrix at in-air AS QPDs.

WFSA, Demod by 36 MHz [W/rad]		
	yaw	pitch
ITMy	-0.257	-0.291
ITMx	0.248	-0.283
BS	-0.213	0.356
PRM	-0.00109	0.00108
PR2	0.00538	-0.00536
PR3	0.0468	0.046717
SRM	-0.000940	0.000868
SR2	-0.00831	-0.00778
SR3	-0.0545	0.051122

Table 17: In-air AS WFSA, demodulated by 36 MHz.

WFSA, Demod by 45MHz [W/rad]		
	yaw	pitch
ITMy	838	585
ITMx	-838	586
BS	813	-817
PRM	0.01524	-0.0101
PR2	-0.0865	-0.0607
PR3	-0.756	0.531
SRM	-0.000710	0.000452
SR2	-0.00534	-0.00340
SR3	-0.0343	0.0218

Table 18: In-air AS WFSA, demodulated by 45 MHz.

WFSB, Demod by 36 MHz [W/rad]		
	yaw	pitch
ITMy	0.949	0.956
ITMx	-0.951	0.958
BS	0.907	-1.31
PRM	0.000791	-0.000829
PR2	-0.00265	0.00280
PR3	-0.0230	-0.0242
SRM	-6.25e-05	7.11e-05
SR2	0.00411	0.00416
SR3	0.0268	-0.0271

Table 19: In-air AS WFSB, demodulated by 36 MHz.

WFSB, Demod by 45MHz [W/rad]		
	yaw	pitch
ITMy	-3460	-2990
ITMx	3470	-2990
BS	-3360	4170
PRM	-0.0470	0.0366
PR2	0.239	-0.186
PR3	2.08	1.61
SRM	0.00113	-0.000837
SR2	0.00848	0.00630
SR3	0.0554	-0.0412

Table 20: In-air AS WFSB, demodulated by 45 MHz.

6 POP DC QPD signal

There is a DC QPD in the POP path to monitor the beam pointing inside PRC [2]. After transmitting PR2, there are two lenses, POPL1 (f =0.333 m) and POPL2 (f =-0.556 m). The ASC matrices at POP QPDs are shown in Table. 21 and 22. The POP signals will be used for the pointing control of the PRC and the signals will be fed back to the beam pointing actuators before PRM. Both POP1 and POP2 are most sensitive to PR3.

QPD1 [W/rad]		
	yaw	pitch
ITMy	-4770	-4180
ITMx	-4770	4190
BS	-4630	5820
PRM	378	-349
PR2	-1510	1360
PR3	-13200	-11900
SRM	-7.44×10^{-6}	6.44×10^{-6}
SR2	-5.60×10^{-5}	-4.85×10^{-5}
SR3	-0.000366	0.000317

Table 21: POP DC QPD1 signal.

QPD2 [W/rad]		
	yaw	pitch
ITMy	5870	5230
ITMx	5870	-5240
BS	5700	-7290
PRM	-211	179
PR2	1850	-1700
PR3	16200	14900
SRM	-1.89×10^{-6}	1.15×10^{-6}
SR2	-1.42×10^{-5}	-8.63×10^{-6}
SR3	-9.29×10^{-5}	5.65×10^{-5}

Table 22: POP DC QPD2 signal.

7 Next steps

Our next step is to create the model in Optickle and to double check the calculation. Also, the signals of the beam pointing towards PRM should be calculated.

For the full interferometer, the strategy for the SRC alignment control should be considered. In our signal extraction scheme, the SRC misalignment signal is difficult to be extracted.

References

[1] LIGO-T1200410-v2, Lisa Barsotti

[2] LIGO-T1000247-v3, Sam Waldman

[3] Internal note by Kiwamu Izumi